

Collision states and scar effects in charged three-body problems

R. Vilela Mendes

Grupo de Física-Matemática

Complexo II, Universidade de Lisboa

Av. Gama Pinto, 2, 1699 Lisboa Codex Portugal

e-mail: vilela@alf4.cii.fc.ul.pt

Abstract

Semiclassical methods form a bridge between classical systems and their quantum counterparts. An interesting phenomenon discovered in this connection is the scar effect, whereby energy eigenstates display enhancement structures resembling the path of unstable periodic orbits.

This paper deals with collision states in charged three-body problems, in periodic media, which are scarred by unstable classical orbits. The scar effect has a potential for practical applications because orbits corresponding to zero measure classical configurations may be reached and stabilized by resonant excitation. It may be used, for example, to induce reactions that are favoured by unstable configurations.

1 Introduction

Classical and quantum mechanics have qualitatively different features. Nevertheless, semiclassical methods[1] provide, in some restricted domains, a bridge between the quantum and classical realms. The Van Vleck-Gutzwiller[2] [3] propagator and the trace formula[4] are landmarks in this connection.

The trace formula relates the fluctuating part of the quantum density of states to an oscillatory sum of exponentials, each term corresponding to

a classical periodic orbit or to one of its multiple retracings. The actual convergence of the periodic orbit sum to the quantum spectrum is still an open question[5]. Nevertheless many interesting results have been obtained by extracting quantum eigenvalue information from the classical periodic orbits[6].

In the trace formula one must sum over all periodic orbits to find a single eigenvalue and in Van Vleck-Gutzwiller propagator $G(q, q', t)$, the momentum uncertainty of the q states implies that trajectories of all energies must be taken into account. This led some authors[7] to suggest that the reliability of the semiclassical results would be improved if one propagates smooth square-integrable wave functions with finite-energy uncertainty. The underlying idea is that the phase-space localized wave functions would filter out the relevant information from the Green's function.

The most interesting wave function information obtained from semiclassical considerations is probably the *scar effect*[8]. For complex systems having phase-space domains with sensitive dependence to initial conditions, periodic orbits are unstable and even when dense they are nevertheless a zero measure set in the smooth ergodic measure. Naively, one would then expect a typical wave function to receive contributions from many orbits and its intensity to reflect the statistical average of them all. If however the intensity of the wave function happens to be either concentrated (or abnormally weak) near a classical periodic orbit one says that *the quantum state is scarred by the periodic orbit*. The occurrence of this behavior is easily understood from a wavepacket propagation argument[8] (see below). It has been observed in numerical calculations of quantum eigenstates of several classically chaotic systems[8] [9] [10] [11] and was related to unstable periodic orbits through semiclassical path integrals[12] [13] [14].

The scar effect may have far-reaching implications for the practical applications of quantum systems. Namely, the unstable classical orbits in chaotic systems, even if dense in phase space, are in practice never observed because all typical motions are aperiodic and uniformly reproduce the support of some diffuse invariant measure. By contrast, in quantum mechanics, whenever an unstable periodic orbit scars a quantum energy eigenstate, the system may easily be made to behave like the unstable orbit by resonant excitation to the corresponding energy level. In this sense scars are a gift of Nature, because they allow the exploration of dynamical configurations that in classical mechanics are washed away by ergodicity. An interesting scar

effect has recently been observed[15] on a semiconductor quantum-well tunneling experiment where, by localizing the probability density, the scarring of the quantum well states increases the overlap with the emitter and leads to enhanced tunnelling for some voltage values.

In this paper I will be concerned with the relevance of the scar effect in accessing collision or near-collision configurations of charged particles in periodic media. Of particular interest are scars associated to separatrix orbits of which a special type, here called *the saddle point scar*, is an example. A simple wave-packet propagation argument[8] qualitatively explains the scar effect. It also allows the derivation of simple conditions which will be important in the interpretation of the scar effects treated in this paper. Consider the overlap integral

$$C(t) = \langle \Psi(t, x) | \Psi(0, x) \rangle \quad (1)$$

for a propagating wave packet which at time zero has a Gaussian shape and initial conditions (p_0, x_0) corresponding to an unstable periodic orbit. Expanding $\Psi(0, x)$ in energy eigenstates

$$\Psi(0, x) = \sum_n c_n \Psi_n(x) \quad (2)$$

one sees that the Fourier transform $S(E)$ of the overlap $C(t)$ is the spectral density weighted by the probabilities $|c_n|^2$.

$$S(E) = \sum_n |c_n|^2 \delta(E - E_n) \quad (3)$$

On the other hand if the period τ of the classical periodic orbit and the largest positive Lyapunov exponent λ are such that $e^{-\tau\lambda/2}$ is not too small, the overlap $C(t)$ will display peaks at times $n\tau$. As the wave packet spreads, the amplitude of the peaks decreases after each orbit traversal at the rate $e^{-\tau\lambda/2}$. The Fourier transform of $C(t)$ will therefore have peaks of width λ with spacing $\omega = \frac{2\pi}{\tau}$. From Eq.(3) one concludes that only the eigenstates that lie under the peaks contribute to the expansion of the wave packet. Since the wave packet has an enhanced intensity along the region of the period orbit, this is expected to carry over to the contributing energy eigenstates. This is the *scar effect*. The stronger the overlap resurgences are, the stronger the effect is expected to be. Therefore the intensity of the effect varies like $1/\tau\lambda$.

This simple derivation[8] of the scar effect is however flawed if the product $\lambda d(E)$ (where $d(E)$ is the mean level density) is very large. Then the number of contributing eigenstates is very large and no individual eigenstate is required to show a significant intensity enhancement near the periodic orbit. Also the argument assumes the low period unstable orbits to be isolated. With many nearby orbits having different periods the argument also breaks down. Conversely, if it happens that in the same configuration space region many different periodic orbits coexist, having the same period, the effect will be enhanced. This is the situation for periodic motions in the neighborhood of an unstable critical point (a saddle) of a potential function $V(x)$. Generically, in the neighborhood of a critical point, there are coordinates where the function may be written as

$$V(x) = \sum_i \frac{1}{2} \sigma_i x_i^2 \quad (4)$$

On the neighborhood of the point $x_i = 0$ there are harmonic periodic motions along the stable directions (positive σ 's) of the critical point. As long as anharmonic corrections are unimportant all the orbits have the same period independently of their amplitude. The instability parameter of these orbits is the smallest negative σ ($\lambda = -|\sigma_{\min}|$). For each positive σ_i the scar intensity factor will be $\frac{1}{\tau\lambda} = \frac{1}{2\pi} \sqrt{\frac{\sigma_i}{\mu}} \frac{1}{|\sigma_{\min}|}$, where μ is the effective mass. The motion in the neighborhood of these unstable periodic orbits being harmonic, the energy of the strongest scar is estimated to be

$$V(0) + E_{loc} + \frac{\hbar}{2} \sqrt{\frac{\sigma_{\max}}{\mu}} \quad (5)$$

where the last term corresponds to the ground state energy of the harmonic motion on the stable direction and E_{loc} is the energy penalty corresponding to the localization energy in the transversal directions. In favorable conditions, that is, if the quadratic approximation for the potential holds over a sufficiently large range, higher energy scars might also be observed corresponding to the excited states of this oscillator. They would have the approximate energy

$$V(0) + E_{loc} + \left(n + \frac{1}{2}\right) \hbar \sqrt{\frac{\sigma_{\max}}{\mu}} \quad (6)$$

In the following two sections we study a one-dimensional and a three-dimensional problem where unstable classical motions indeed leave their trace in the some of the quantum states. Of particular interest here are the unstable classical motions which correspond to collision or almost-collision configurations. Some of the potential practical applications of this effect are discussed in the conclusions.

2 Scarred collision states in a one-dimensional periodic problem

Let a quantum system be described by the Hamiltonian

$$H_1 = -\frac{\partial^2}{\partial x_1^2} - \frac{\partial^2}{\partial x_2^2} - \frac{1}{\gamma} \frac{\partial^2}{\partial y^2} + V(|x_1 - x_2|) - V(|x_1 - y|) - V(|x_2 - y|) \quad (7)$$

with periodic boundary conditions on a lattice of lattice size L . The Hamiltonian represents a many-body system with two heavy and one light particle (γ of order 10^{-4} , for example) in each lattice cell and periodic boundary conditions or, alternatively, a three-particle system living on the circle. The heavy particles repel each other and attract the light one. For definiteness I have considered the heavy particles to be positively charged and the light particle to be the negative one. The interaction potential is

$$V(x) = \frac{g}{2L} \left(1 + \cos(2\pi \frac{x}{L}) \right) \quad (8)$$

The factor $\frac{1}{L}$ is included in the coupling constant $\frac{g}{L}$ as a convenient factorization in case one wants to insure scaling properties similar to the three-dimensional Coulomb problem. Periodic boundary conditions are imposed on the quantum problem by choosing a basis of box-normalized momentum eigenstates with periodic boundary conditions $\frac{1}{\sqrt{L}} \exp(i2\pi kx)$, $k = \frac{n}{L}$, $n = 0, \pm 1, \pm 2, \dots$. Denote by $|n_1 n_2 p\rangle$ a state with momenta $\frac{n_1}{L}$, $\frac{n_2}{L}$ and $\frac{p}{L}$ respectively. The matrix elements of H_1 in this basis are

$$\begin{aligned} \langle n'_1 n'_2 p' | H_1 | n_1 n_2 p \rangle = & \delta_{n'_1 n_1} \delta_{n'_2 n_2} \delta_{p' p} (2\pi)^2 \frac{1}{L^2} \left(n_1^2 + n_2^2 + \frac{p^2}{\gamma} \right) \\ & + \frac{g}{L} \delta_{pp} \delta(n_1 - n'_1 + n_2 - n'_2) f_1(n_1 - n'_1 - n_2 + n'_2) \\ & - \frac{g}{L} \delta_{n'_2 n_2} \delta(n_1 - n'_1 + p - p') f_1(n_1 - n'_1 - p + p') \\ & - \frac{g}{L} \delta_{n'_1 n_1} \delta(p - p' + n_2 - n'_2) f_1(p - p' - n_2 + n'_2) \end{aligned} \quad (9)$$

where f_1 is the function

$$f_1(\alpha) = \frac{1}{4} (2\delta_{\alpha,0} + \delta_{\alpha,2} + \delta_{\alpha,-2}) \quad (10)$$

The center of mass motion is separated by changing coordinates to

$$\begin{aligned} R &= \frac{1}{2+\gamma} (x_1 + x_2 + \gamma y) \\ r &= x_1 - x_2 \\ \eta &= y - \frac{x_1 + x_2}{2} \end{aligned} \quad (11)$$

Classically the dynamics in the center of mass of the three particles is ruled by the Hamilton equations

$$\begin{aligned} \dot{r} &= 4p_r \\ \dot{p}_r &= -gV'(r) + \frac{1}{2}gV'(\frac{r}{2} - \eta) - \frac{1}{2}gV'(-\frac{r}{2} - \eta) \\ \dot{\eta} &= \frac{2+\gamma}{\gamma}p_\eta \\ \dot{p}_\eta &= -g \left\{ V'(\frac{r}{2} - \eta) + V'(-\frac{r}{2} - \eta) \right\} \end{aligned} \quad (12)$$

That is, the center of mass dynamics is equivalent to the motion of a two dimensional particle in the potential

$$U(r, \eta) = g \left\{ V(r) - V(\frac{r}{2} - \eta) - V(-\frac{r}{2} - \eta) \right\} \quad (13)$$

with an effective Hamiltonian

$$H_{CM} = 2p_r^2 + \frac{2+\gamma}{2\gamma}p_\eta^2 + U(r, \eta) \quad (14)$$

The potential $U(r, \eta)$ is displayed in Fig.1 with r and η in units of L . It has two stable minima at $(r = \frac{L}{3}, \eta = 0)$ ($r = -\frac{L}{3}, \eta = 0$) and a saddle point at $(r = \eta = 0)$. The minima correspond to configurations with the two positive particles well separated and the negative one midway between the other two. The saddle point is a collision state of the two heavy positive particles which however has relatively low energy because the repulsive energy of the positive particles is compensated by the attractive interaction with the negative one. In addition to the unstable fixed point at $r = \eta = 0$ there is a whole collection of unstable periodic orbits along the $r = 0$ axis. According to (5), the energy of the corresponding saddle point scar is estimated to be

$$E_s \simeq -\frac{g}{L} + E_{loc} + \frac{1}{2} \sqrt{\frac{4g\pi^2(2+\gamma)}{\gamma L^3}} \quad (15)$$

In case one wants to use scar effects to induce collisions the important quantity to know is the difference between E_s and the ground state energy. The structure of the ground state will depend on the order of magnitude of the physical parameters. For definiteness I assume the ratio of negative to the positive particles mass to be very small ($O(10^{-4})$) and also of order L^{-1} in the natural units used to write Eq.(7). For the numerical results shown below the values used are $\gamma = 2.7 \times 10^{-4}$, $L = 13039$ and $g = 6$.

From (9) one sees that to excite the first kinetic mode of the light particle one needs an energy $\frac{(2\pi)^2}{L^2\gamma}$ as compared to kinetic energies of order $\frac{(2\pi)^2}{L^2}$ needed to localize the heavy particles. Therefore one expects the ground state to have a completely delocalized light particle and a heavy particle relative coordinate localized around $\frac{L}{2}$. For this configuration both the transversal localization energy and the potential energy are similar to those for the scar in (15). Therefore

$$\Delta_s = E_s - E_0 \simeq \frac{1}{2} \sqrt{\frac{4g\pi^2(2+\gamma)}{\gamma L^3}} \quad (16)$$

A numerical diagonalization of the scaled LH_1 Hamiltonian of Eq.(7) was performed on a basis of 729 states restricted to zero total momentum (center of mass configurations). The structure of the energy spectrum is shown in Fig.2. The band structure corresponds to the energies needed to excite the successively higher kinetic modes of the light particle. The first state in each band lies approximately at the energy

$$E_0 + n^2 \frac{(2\pi)^2}{\gamma L}$$

$n = 0, 1, 2, \dots$. The ground state energy is $E_0 = -5.91$. The amplitude of the ground state wave function is shown in Fig.3. The amplitude of the state at the top of the negative energy band ($E_s = -0.905$) is shown in Figs.4a,b. This is the state that corresponds to the saddle point scar described above. The difference $E_s - E_0$ is 5.01 to be compared with the value 5.8 obtained from the analytical estimate (16). The state, at the top of the first band, is, in this band, the one with the largest *heavy particle overlap*, defined as

$$\int |\Psi(0, \eta)|^2 d\eta$$

For other bands it also happens that the state with the largest overlap is at the top of the band. I do not know whether there is a general mechanism leading to this fact or whether it is a particular feature of this model. There are in each band other states with large overlaps which however, as a rule, are not so concentrated along the $r = 0$ line (see for example in Fig.5 the contour plot for the state at $E = -1.298$).

In this system, the harmonic approximation used in (5) to predict the first scar state energy, cannot be reliably carried over to higher harmonic excitations, because higher energy states are not so localized around ($r = \eta = 0$) and the quadratic approximation for the potential is no longer valid. For example for the state at the top of the second band (Fig.6) we have $E - E_0 = 18.67$ whereas (6) with $n = 1$ would predict 17.4. For the state at the top of the third band (Fig.7), $E - E_0 = 51.22$ whereas (6) with $n = 2$ yields 29.0.

3 A three-dimensional periodic Coulomb problem

The three-dimensional problem considered here is, as before, a periodic boundary condition many-body problem with two heavy and one light particle in each lattice cell of volume L^3 or, alternatively, a three-particle system living on the 3-torus. The interaction is the Coulomb potential

$$V(|x_1 - x_2|) = \frac{1}{|x_1 - x_2|} \quad (17)$$

In problems with periodic boundary conditions and long-range interactions it would make sense to consider that, acting on the particles in one cell, are the forces of all the particles in the other cells or at least of those on the neighboring cells. Alternatively one might change the potential to make it L -periodic.

Here periodicity is explicitly introduced by the choice of a periodic basis of momentum eigenstates as in the one-dimensional problem. However for the computation of the matrix elements of the Hamiltonian only the forces between the three particles will be considered. This slightly underestimates the interaction part of the Hamiltonian but it does not change the qualitative

nature of the problem especially in what concerns the small distance collision effects.

For this problem I will first find the low-lying quantum spectrum and then see whether the strong overlap states may or may not be interpreted as scar states. In a basis of momentum eigenstates $|\vec{n}_1 \vec{n}_2 \vec{p}\rangle$ with $|n\rangle = (L)^{-\frac{3}{2}} \exp(i\frac{2\pi}{L} \vec{n} \cdot \vec{x})$, the matrix elements of the Hamiltonian

$$H_2 = -\Delta_1 - \Delta_2 - \frac{1}{\gamma} \Delta_3 + |x_1 - x_2|^{-1} - |x_1 - y|^{-1} - |x_2 - y|^{-1} \quad (18)$$

are

$$\begin{aligned} \left\langle \vec{n}_1 \vec{n}_2 \vec{p} \left| H_2 \right| \vec{n}_1 \vec{n}_2 \vec{p} \right\rangle &= \delta_{\vec{n}_1 \vec{n}_1}^{\vec{n}_1 \vec{n}_1} \delta_{\vec{n}_2 \vec{n}_2}^{\vec{n}_2 \vec{n}_2} \delta_{\vec{p} \vec{p}}^{\vec{p} \vec{p}} (2\pi)^2 \frac{1}{L^2} \left(|n_1|^2 + |n_2|^2 + \frac{|\vec{p}|^2}{\gamma} \right) \\ &+ \frac{1}{L} \delta_{\vec{p} \vec{p}}^{\vec{p} \vec{p}} \delta^3(\vec{n}_1 - \vec{n}_1 + \vec{n}_2 - \vec{n}_2) f_2(|\vec{n}_1 - \vec{n}_1 - \vec{n}_2 + \vec{n}_2|) \\ &- \frac{1}{L} \delta_{\vec{n}_2 \vec{n}_2}^{\vec{n}_2 \vec{n}_2} \delta^3(\vec{n}_1 - \vec{n}_1 + \vec{p} - \vec{p}) f_2(|\vec{n}_1 - \vec{n}_1 - \vec{p} + \vec{p}|) \\ &- \frac{1}{L} \delta_{\vec{n}_1 \vec{n}_1}^{\vec{n}_1 \vec{n}_1} \delta^3(\vec{p} - \vec{p} + \vec{n}_2 - \vec{n}_2) f_2(|\vec{p} - \vec{p} - \vec{n}_2 + \vec{n}_2|) \end{aligned} \quad (19)$$

with

$$f_2(|\alpha|) = \frac{1}{2\pi |\alpha|} (1 - \cos(\pi \rho |\alpha|)) \quad (20)$$

and $\rho = 2 \left(\frac{3}{4\pi} \right)^{\frac{1}{3}}$. For the computation of the spectrum of H_2 one considers also states symmetric and antisymmetric under interchange of the two heavy particles.

$$|\vec{n}_1 \vec{n}_2 \vec{p}\rangle_{\pm} = \frac{1}{c} (|\vec{n}_1 \vec{n}_2 \vec{p}\rangle \pm |\vec{n}_1 \vec{n}_2 \vec{p}\rangle) \quad (21)$$

with $c = \sqrt{2}$ for $\vec{n}_1 \neq \vec{n}_2$ and $c = 2$ for $\vec{n}_1 = \vec{n}_2$. For the numerical diagonalization of the Hamiltonian H_2 a basis of 3176523 states was considered. Using momentum conservation and conservation of permutation symmetry type the matrix is however reduced into invariant blocks to simplify the computation. Fig.8 shows the lower part of the spectrum for center of mass (zero total momentum) states with symmetric states denoted by crosses and antisymmetric ones by dots. In Figs.9a and 9b one compares the lowest lying antisymmetric (Ψ_{0a}) and symmetric (Ψ_{0s}) states. The quantity that is

plotted is the integrated probability

$$|\Psi(|r|, |\eta|)|^2 = \int d\Omega_r d\Omega_\eta |\Psi(r, \eta)|^2 \quad (22)$$

The lowest lying symmetric eigenstate displays a strong overlap of the heavy particles. The nature of this state is better understood from the two-coordinate projections

$$|\Psi(r_i, \eta_j)|^2 = \int d^2r d^2\eta |\Psi(r, \eta)|^2 \quad (23)$$

the integration being carried over all coordinates other than r_i and η_j . Figs.10a and 10b show $|\Psi(r_1, \eta_1)|^2$ and $|\Psi(r_1, \eta_2)|^2$. All other like-coordinate and unlike-coordinate projections are identical to those shown in the figures.

As in the one-dimensional case studied before, there is a simple relation between this state and classical orbits. The classical equations for center of mass motion are

$$\begin{aligned} \dot{\vec{r}} &= 4\vec{p}_r \\ \dot{\vec{p}}_r &= \vec{r} |r|^{-3} - \frac{1}{2} \left(\frac{\vec{r}}{2} - \vec{\eta} \right) \left| \frac{\vec{r}}{2} - \vec{\eta} \right|^{-3} - \frac{1}{2} \left(\frac{\vec{r}}{2} + \vec{\eta} \right) \left| \frac{\vec{r}}{2} + \vec{\eta} \right|^{-3} \\ \dot{\vec{\eta}} &= \frac{2+\gamma}{\gamma} \vec{p}_\eta \\ \dot{\vec{p}}_\eta &= \left(\frac{\vec{r}}{2} - \vec{\eta} \right) \left| \frac{\vec{r}}{2} - \vec{\eta} \right|^{-3} - \left(\frac{\vec{r}}{2} + \vec{\eta} \right) \left| \frac{\vec{r}}{2} + \vec{\eta} \right|^{-3} \end{aligned} \quad (24)$$

For collisions or near-collisions to take place at low energies the light particle must be near the two heavy particles part of the time in order for the attractive energy to compensate the strong repulsion. This implies some localization of the light particle in one dimension at least. Localization in more dimensions however is very costly in kinetic energy. Therefore it is likely to find, associated to the low lying symmetric state, orbits corresponding to planar motion but not to collinear motion. From (24) it follows that there are orbits in the plane (r_1, η_2) , that is, if at $t = 0$ one has $r_2 = p_{r2} = r_3 = p_{r3} = \eta_1 = p_{\eta1} = \eta_3 = p_{\eta3} = 0$ then the same holds true for all t . The phase-portrait in the plane (r_1, η_2) is symmetric about the $r_1 = 0$ line. In Fig.11a and 11b I have plotted two typical orbits. Periodic boundary conditions are imposed at $\frac{1}{2}$ and $-\frac{1}{2}$. In-between the orbits that move to the right and to the left there is the separatrix at $r_1 = 0$ that passes through the singular point of the potential. It is precisely along this separatrix that the

state Ψ_{0s} is strongly scarred. In this case we have not found a saddle scar in the sense defined in the introduction because the separatrix goes through a singular point of the potential. It is possible that by a change of time, and using the well-known regularization[16] of the Kepler problem one may still be able to formally interpret the state as a saddle scar. This is not however very important. What is important to notice is that once again we have found that the low-energy collisional state is associated to an unstable feature of the classical phase-portrait.

4 Conclusions

Through the scar effect, orbits that correspond to zero measure classical configurations may be reached and stabilized in quantum mechanics by resonant excitation with the appropriate energy. Their location in the energy spectrum may, in favorable cases, be found either from theoretical considerations (from symmetry, from being at the top of bands, etc.) or from absorption experiments.

This characteristically quantum phenomenon, may be practically used to induce reactions which are favored by unstable or difficult to reach configurations. An obvious potential application is to fusion reactions. Most practical nuclear fusion mechanisms proposed so far have a two-mechanism nature. For example muon catalyzed fusion relies on the fact that the muon is 200 times heavier than the electron to bring the bound nuclei together, but then it is the tunneling effect that will eventually allow the nuclei to fuse. In toroidal plasma confinement it is the magnetic field configuration that keeps the ions together, but then it is radio frequency or ion injection heating that supplies them with enough kinetic energy to overcome the Coulomb barrier. What I am proposing here is that if enough deuterons, for example, are confined in a periodic medium (a crystal lattice, for example) then, resonant excitation and the scar effect may be used to excite collisional states and induce fusion reactions. I strongly emphasize that like in the known fusion methods we should separate the two problems of confinement and collision. The crystal lattice only serves as a confinement device, an additional collision mechanism being needed, which the scar effect, discussed in this paper, may provide. This is contrary to the hopes of the cold fusion saga where spontaneous fusion was expected just from confining deuterons in a lattice.

Actually a simple calculation shows that in the problem discussed in Section 3 the separation between the ground state and the first scar state is such that thermal excitation is highly improbable. However resonant excitation by electromagnetic radiation seems possible.

For other applications of the scar effect and in particular of its saddle point enhancement one might think of catalyzing chemical reactions on lattice substrates.

In conclusion: unstable configurations corresponding to unstable periodic orbits are in classical mechanics of little use unless very sophisticated control methods are used[17]. This is because, for each energy level, the stable invariant measures are smoothly distributed all over the energy surface. In this sense quantum mechanics is more parsimonious because for each energy level it displays just a fraction of the blurred picture of smooth classical dynamics. In particular, by isolating through the scar effect improbable classical configurations, quantum mechanics is, for practical applications, a cure to the classical mechanics curse of ergodicity on the energy surface.

5 Figure captions

- Fig.1 - Effective center of mass potential for the one-dimensional problem
- Fig.2 - Energy spectrum in the one-dimensional problem
- Fig.3 - Ground state wave function
- Figs.4a,b - Wave function of the state at the top of the negative energy band
- Fig.5 - Contour plot for the state at energy $E = -1.298$
- Fig.6 - Wave function of the state at the top of the second energy band
- Fig.7 - Wave function of the state at the top of the third energy band
- Fig.8 - Energy spectrum in the three-dimensional problem
- Figs.9a,b - $|\Psi(|r|, |\eta|)|^2$ for the lowest lying antisymmetric and symmetric states
- Fig.10a - $|\Psi(r_1, \eta_1)|^2$ for the lowest lying symmetric state
- Fig.10b - $|\Psi(r_1, \eta_2)|^2$ for the lowest lying symmetric state
- Figs.11a,b - Two classical center of mass orbits in the plane (r_1, η_2)

References

- [1] V. P. Maslov and M. V. Fedoriuk; *Semiclassical approximations in quantum mechanics*, Reidel, Dordrecht 1981.
- [2] J. H. Van Vleck; Proc. Natl. Acad. Sci. 14 (1928) 178.
- [3] M. C. Gutzwiller; J. Math. Phys. 8 (1967) 1979.
- [4] M. C. Gutzwiller; J. Math. Phys. 12 (1971) 343.
- [5] A. Voros; J. Phys. A21 (1988) 685.
- [6] M. C. Gutzwiller; Physica 5D (1982) 183 ; P. Cvitanovic and B. Eckardt, Phys. Rev. Lett. 63 (1989) 823 ; M. Sieber and F. Steiner, Physica D44 (1990) 248 ; M. V. Berry and J. P. Keating, J. Phys. A23 (1990) 4839 ; G. Tanner et al. , Phys. Rev. Lett. 67 (1991) 2410 ; S. Tomsovic, M. Grinberg and D. Ullmo, Phys. Rev. Lett. 75 (1995) 4346 ; E. B. Bogomolny and J. P. Keating, Phys. Rev. Lett. 77 (1996) 1472.
- [7] S. Tomsovic and E. J. Heller; Phys. Rev. E47 (1993) 282.
- [8] E. J. Heller; Phys. Rev. Lett. 53 (1984) 1515 and in *Chaos and Quantum Physics*, M. J. Giannoni, A. Voros and J. Zinn-Justin (Eds.) Elsevier, Amsterdam 1991.
- [9] S. W. McDonald; Lawrence Berkeley Lab. Report LBL-14837.
- [10] R. D. Taylor and P. Brumer; Faraday Discuss. Chem. Soc. 75 (1983) 170.
- [11] M. Saraceno; Ann. Phys. 199 (1990) 37.
- [12] E. B. Bogomolny; Physica D31 (1988) 169.
- [13] M. V. Berry; Proc. Roy. Soc. London A423 (1989) 219.
- [14] M. Feingold, R. G. Littlejohn, S. B. Solina, J. S. Pehling and O. Piro; Phys. Lett. A146 (1990) 199.
- [15] P. B. Wilkinson et al.; Nature 380 (1996) 608.
- [16] P. Kustaanheimo and E. Stiefel; J. Reine Angew. Math. 218 (1965) 204.
- [17] E. Ott, C. Grebogi and J. A. Yorke; Phys. Rev. Lett. 64 (1990) 1196.

This figure "fig1.gif" is available in "gif" format from:

<http://arxiv.org/ps/quant-ph/9705040v1>

Fg2

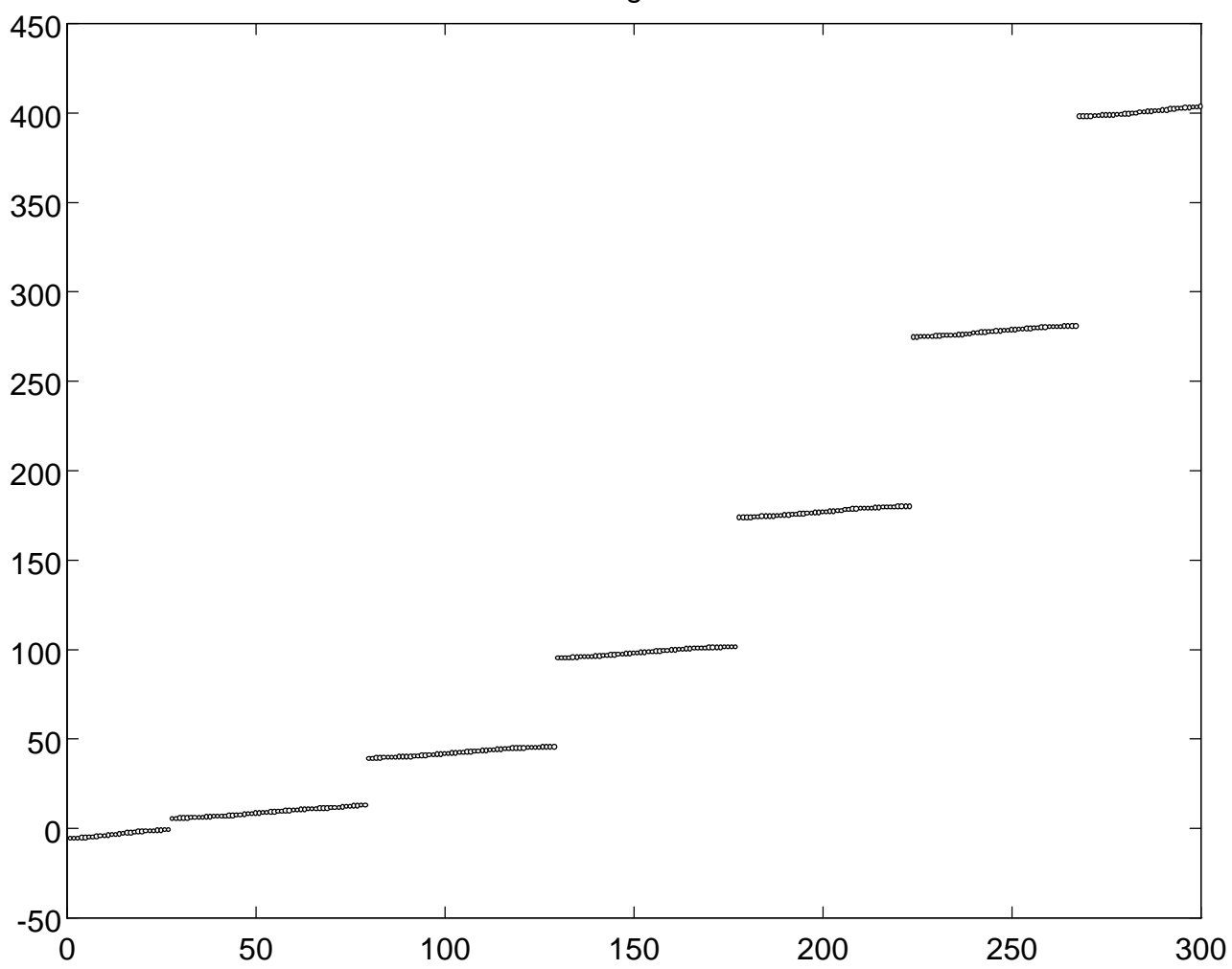


Fig . 3

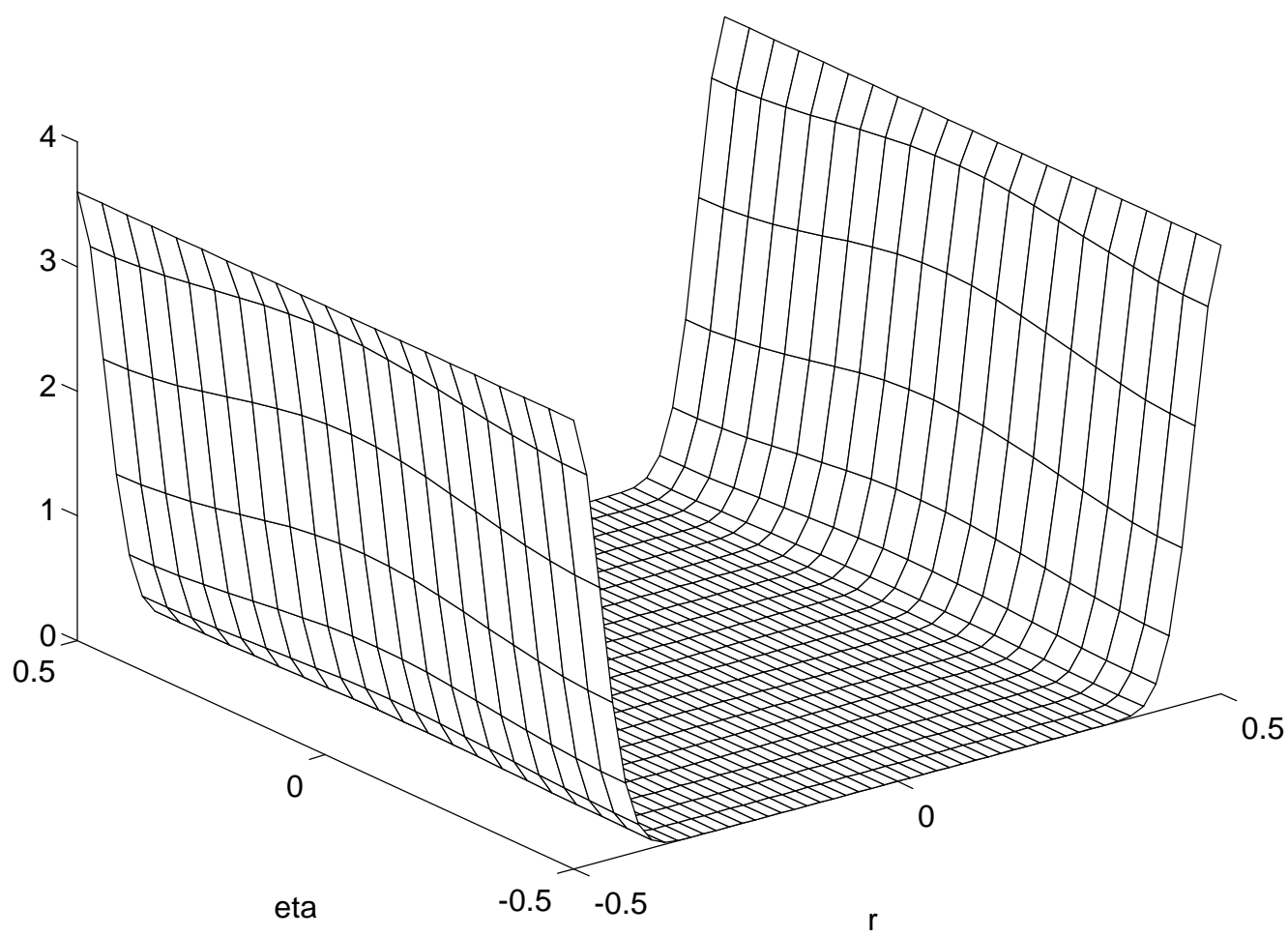


Fig . 4 a

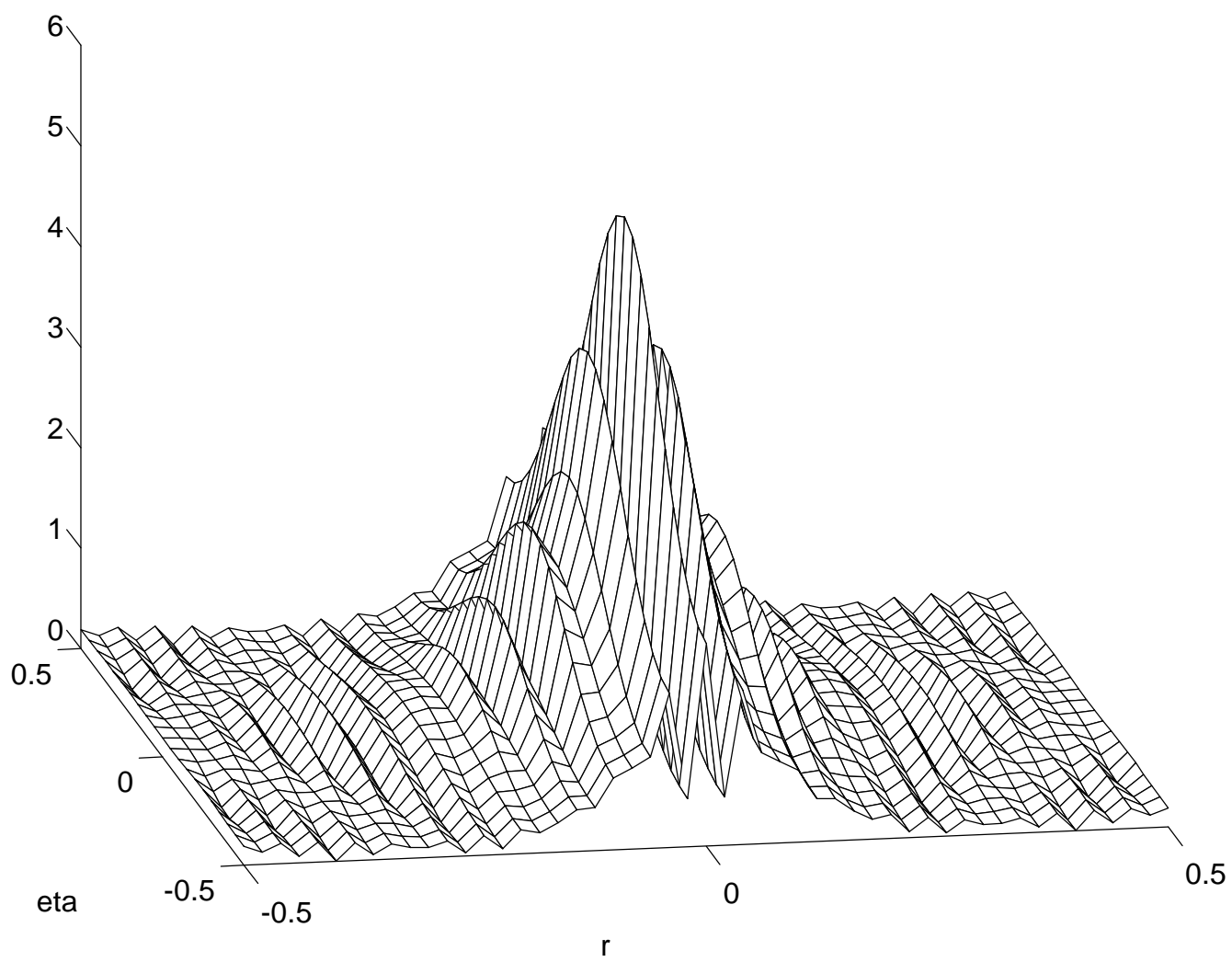


Fig . 4 b

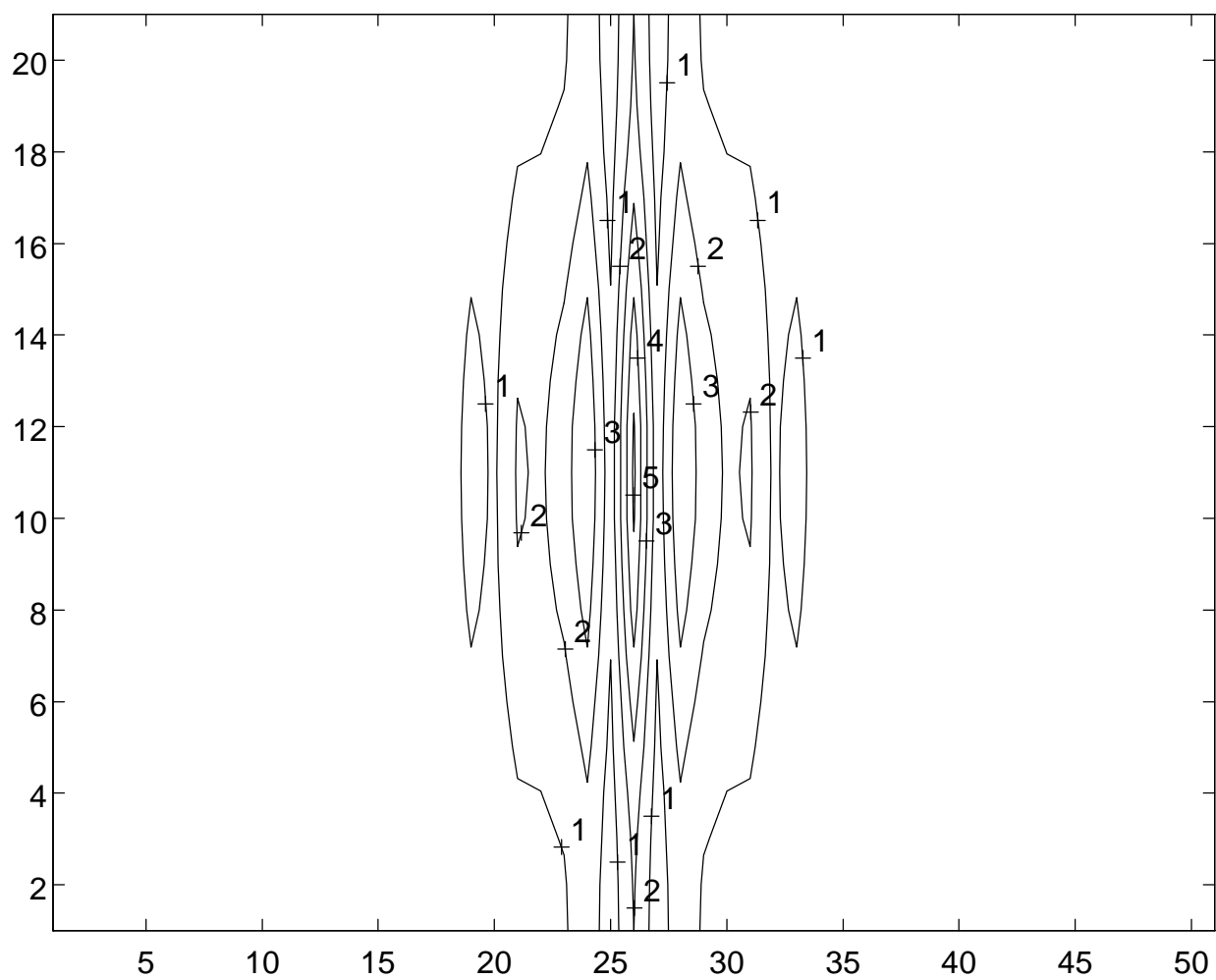


Fig . 5

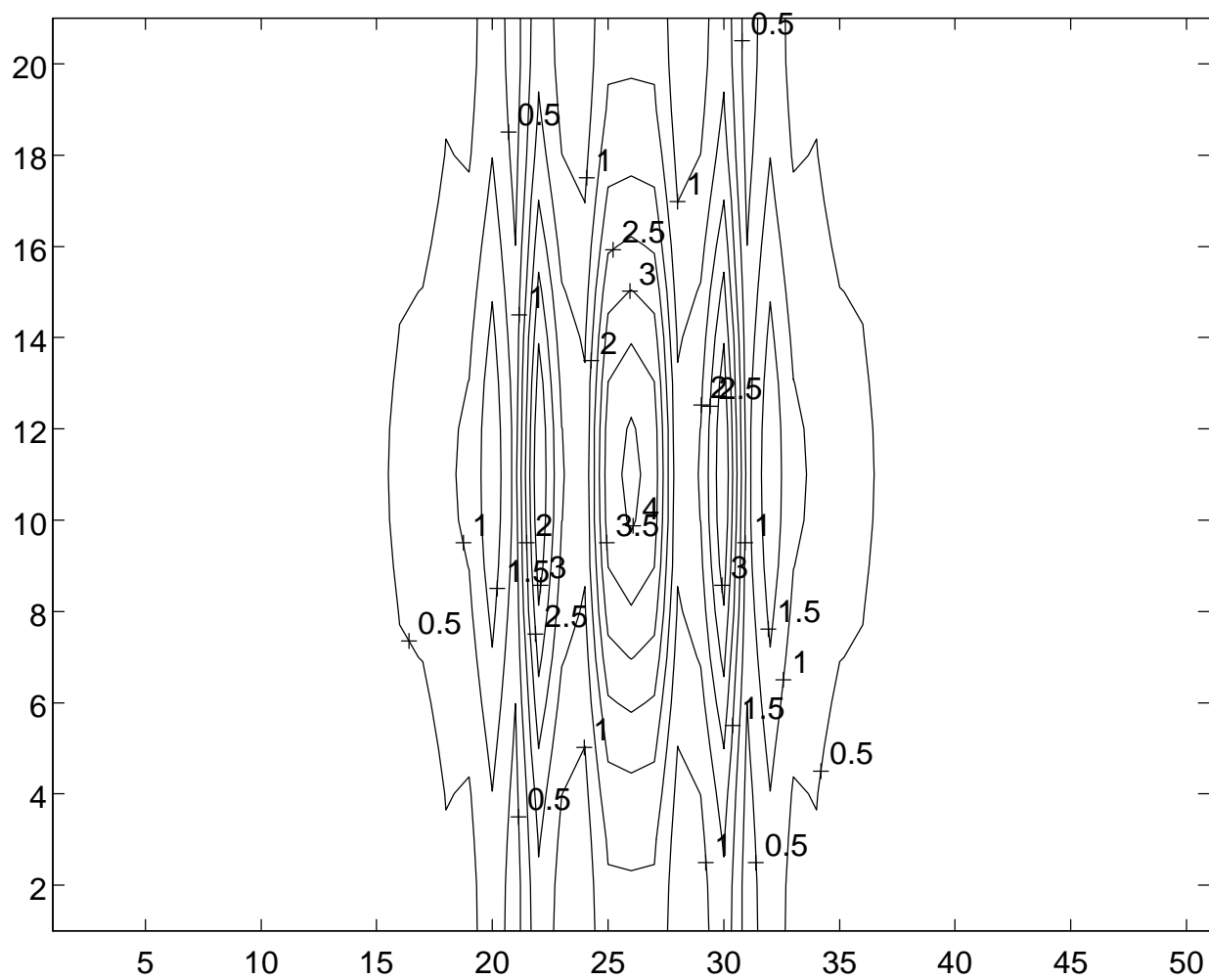
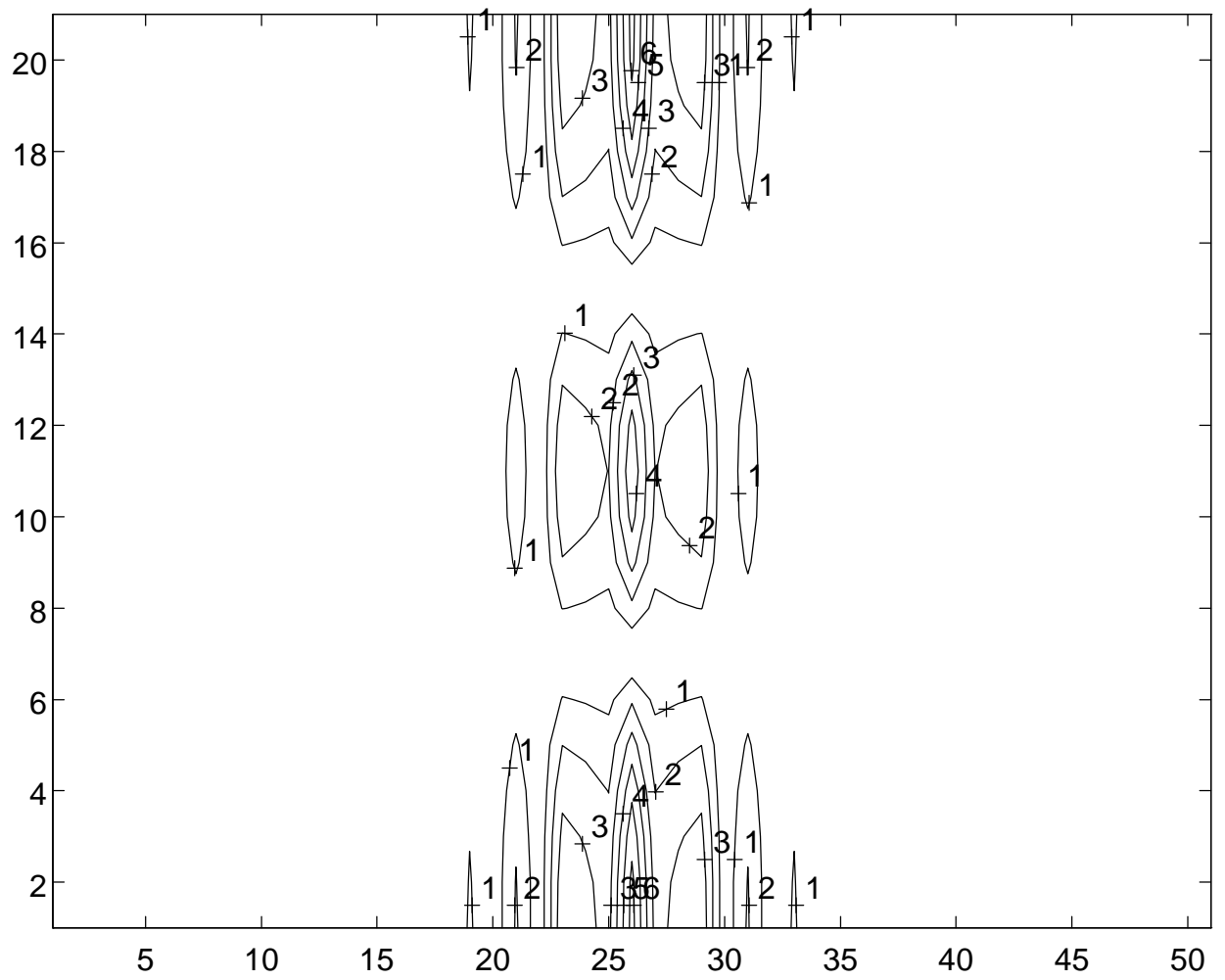


Fig . 6



F i g . 7

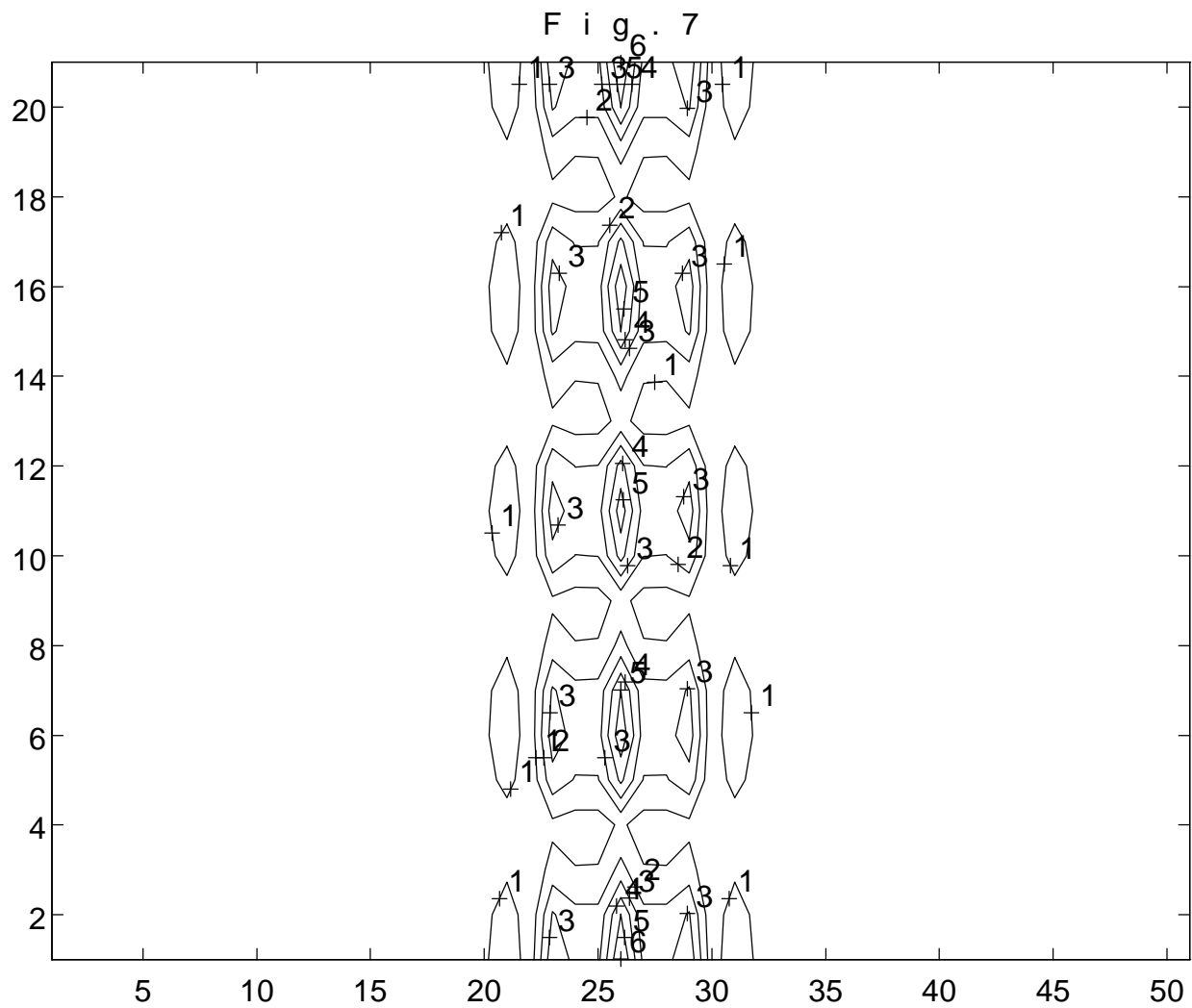


Fig.8

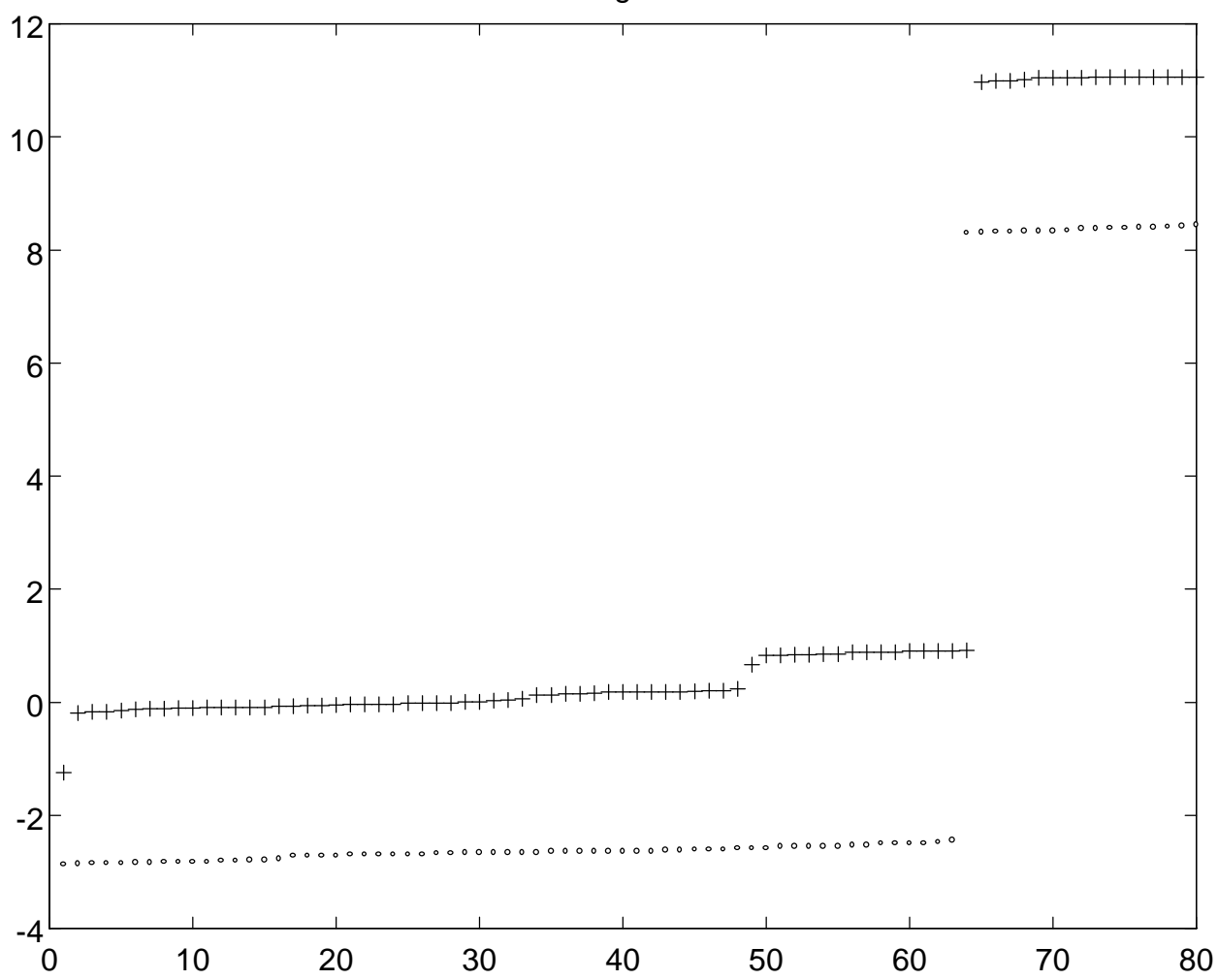


Fig.9a

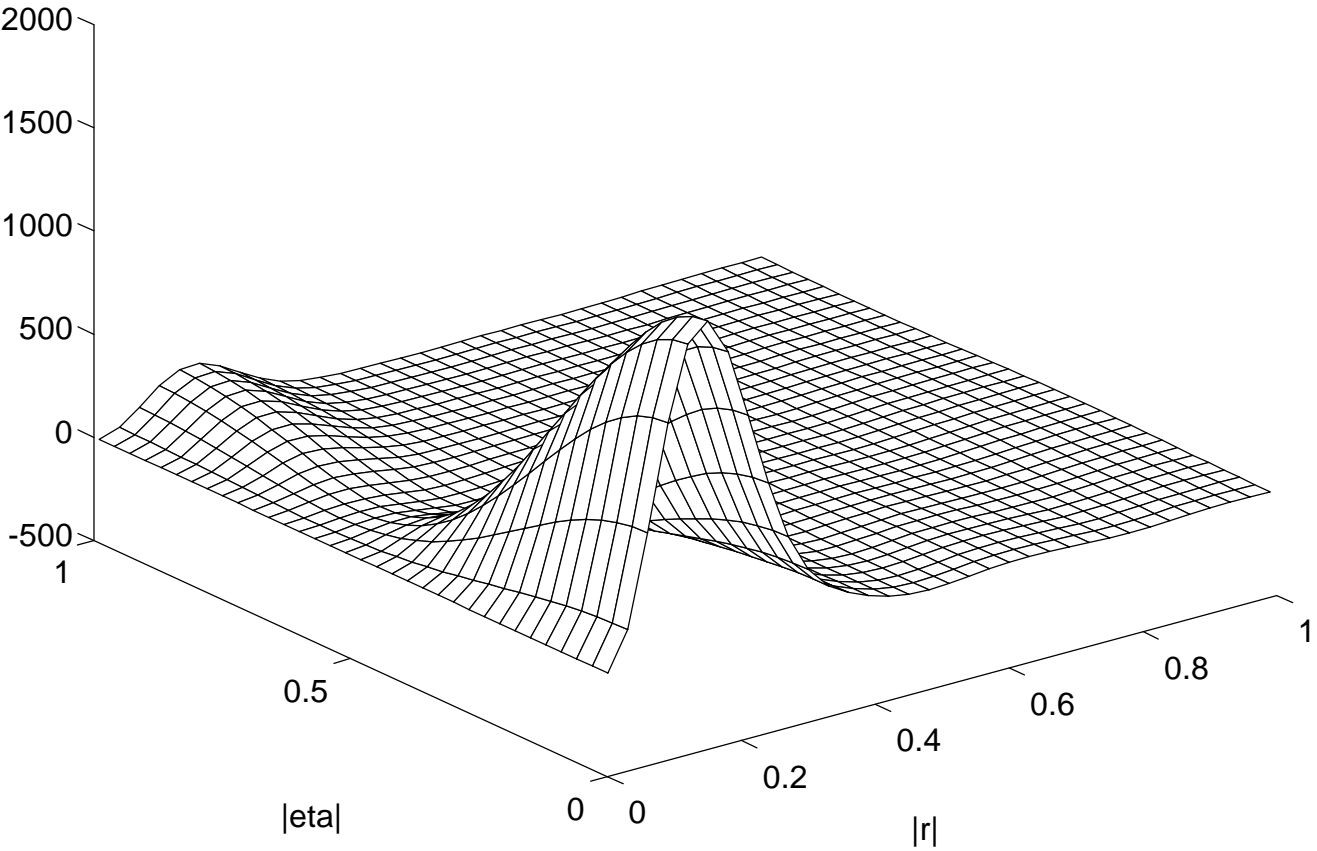


Fig.9b

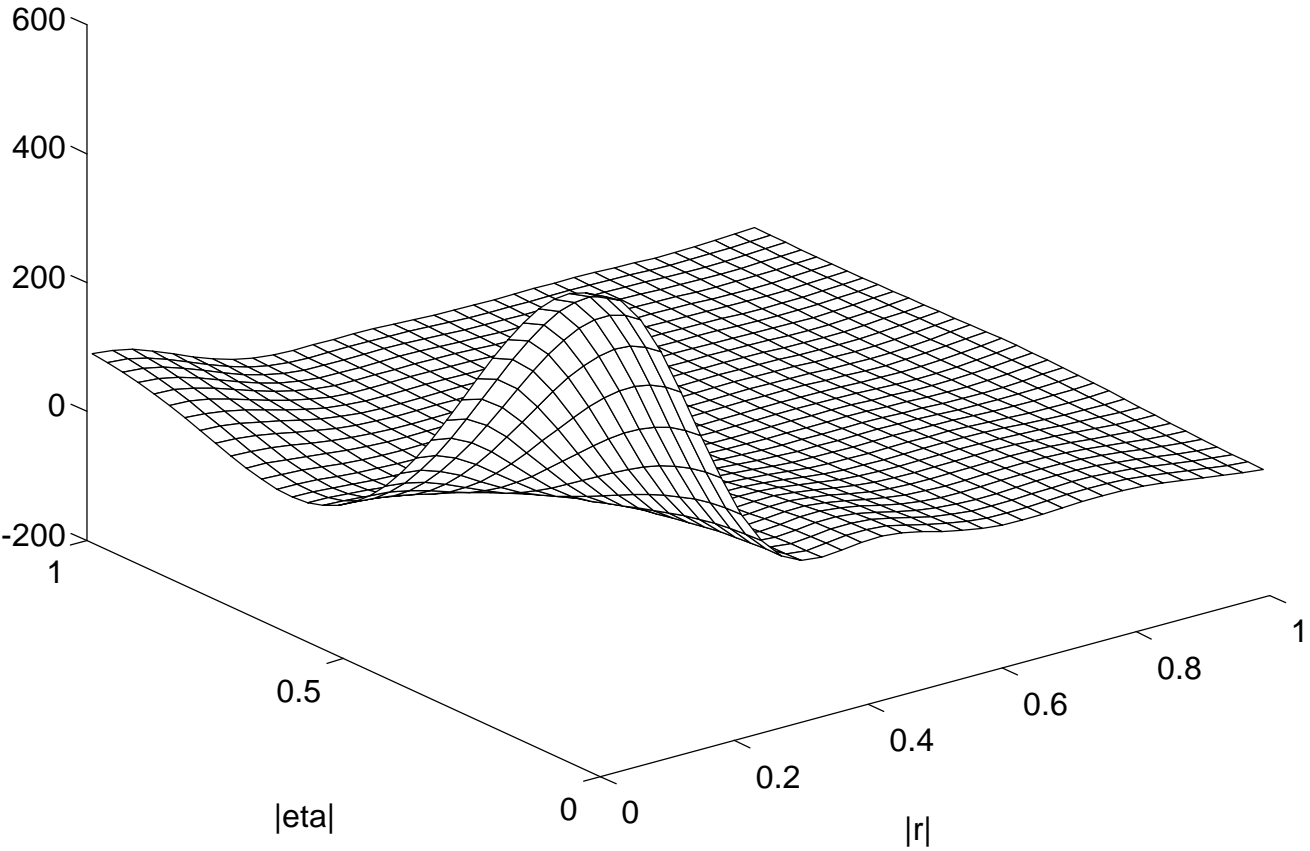


Fig.10a

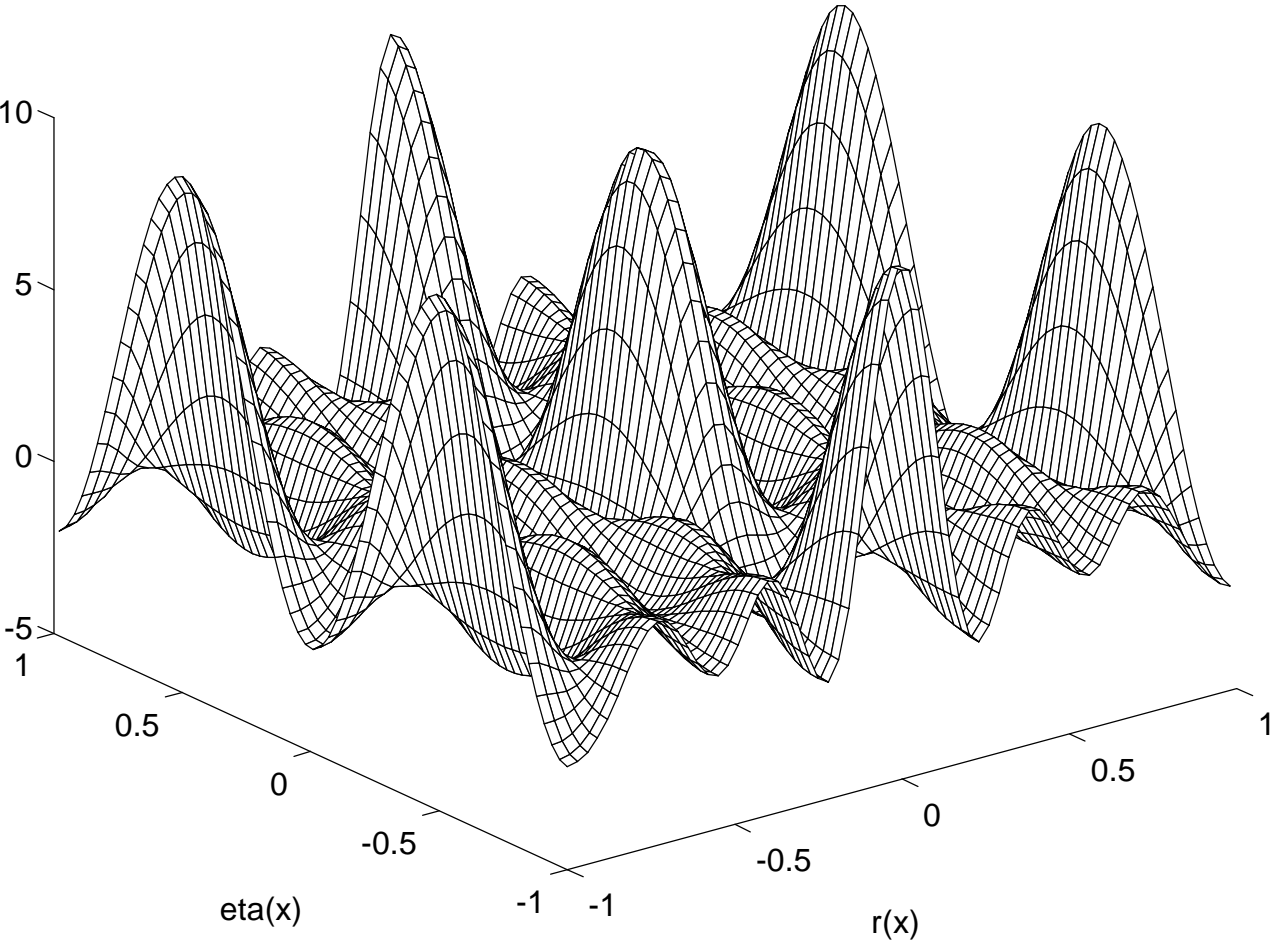


Fig.10b

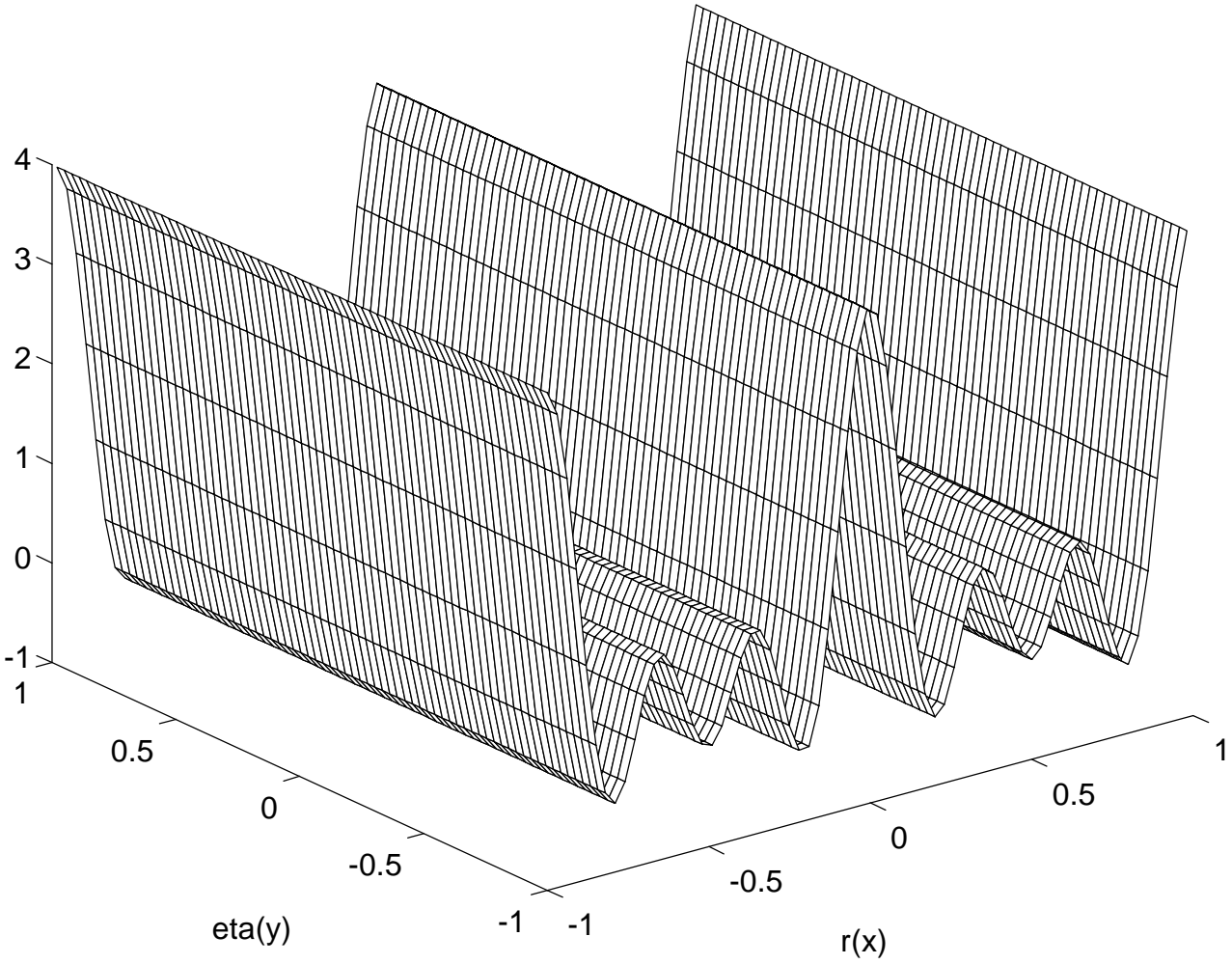


Fig.11a

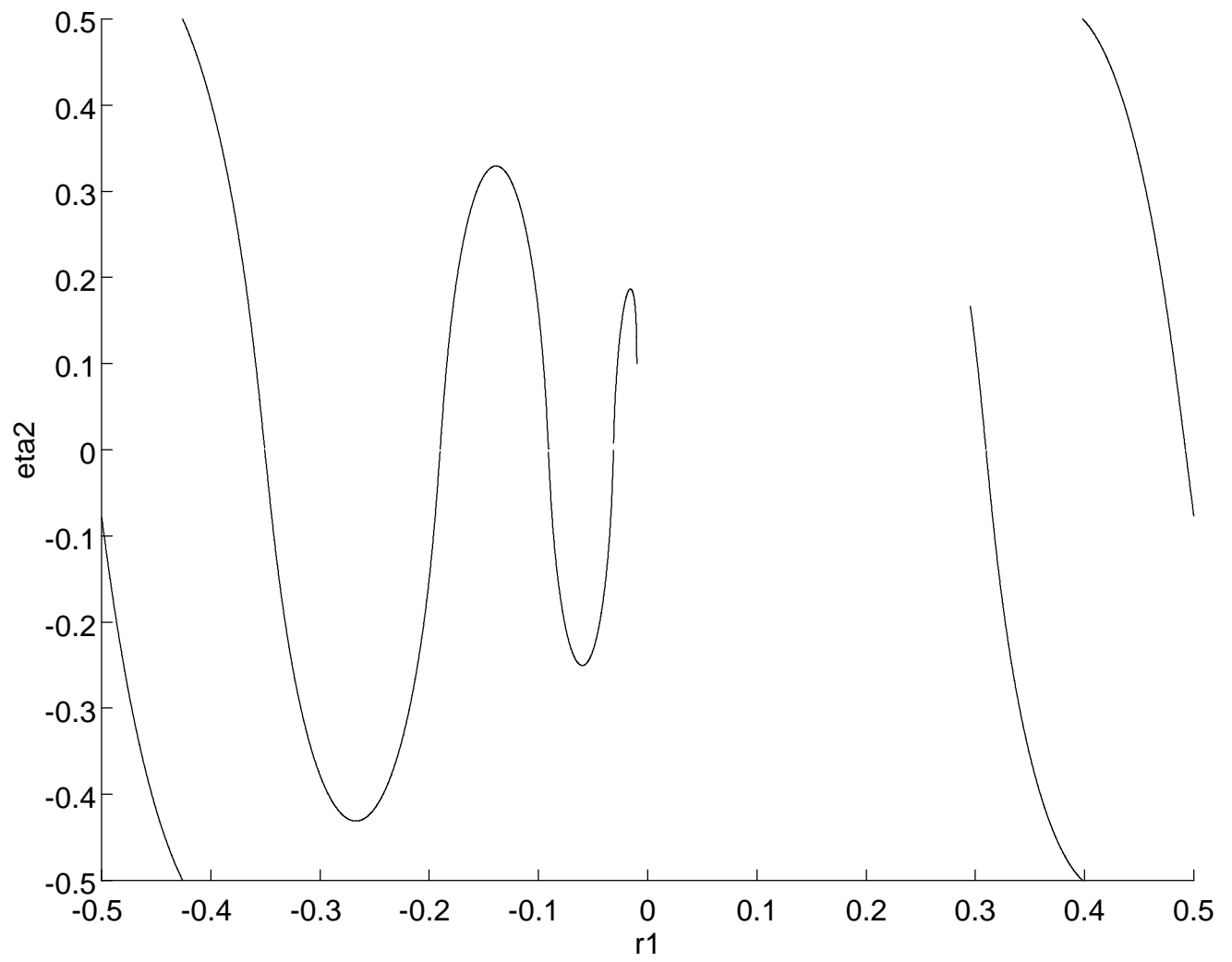


Fig.11b

